Precision Engineering 62 (2020) 265–272

Contents lists available at ScienceDirect

Precision Engineering

journal homepage: http://www.elsevier.com/locate/precision

Plane kinematic calibration method for industrial robot based on dynamic measurement of double ball bar

Ping Yang *, Zhiguang Guo, Yangbo Kong

Department of Mechanical and Electrical Engineering, School of Aerospace Engineering, Xiamen University, Xiamen, 361102, China

ARTICLE INFO

Keywords:
Dynamic measurement
DBB
Sub-plane
Industrial robot
Roundness error
Laser interferometer

ABSTRACT

A new calibration method is proposed to improve the circular plane kinematic accuracy of industrial robot by using dynamic measurement of double ball bar (DBB). The kinematic model of robot is established by the MDH (Modified Denavit-Hartenberg) method. The error mapping relationship between the motion error of end-effector and the kinematic parameter error of each axis is calculated through the Jacobian iterative method. In order to identify the validity of the MDH parameter errors, distance errors and angle errors of each joint axis were simulated by three orders of magnitude respectively. After multiple iterations, the average value of kinematic error modulus of end-effector was reduced to nanometer range. Experiments were conducted on an industrial robot (EPSON C4 A901) in the working space of 180 mm × 490 mm. Due to the measuring radius of DBB, the working space was divided into 30 sub-planes to measure the roundness error before and after compensation. The average roundness error calibrated by the proposed method at multi-planes decreased about 21.4%, from 0.4637 mm to 0.3644 mm, while the standard deviation of roundness error was reduced from 0.0720 mm to 0.0656 mm. In addition, by comparing the results of positioning error measured by the laser interferometer before and after calibration, the range values of motion errors of end-effector were decreasing by 0.1033 mm and 0.0730 mm on the X and Y axes, respectively.

1. Introduction

Kinematic accuracy of industrial robot is a key factor that constrains its performance in high precision industrial applications. The kinematic calibration of robot is an effective process to improve the accuracy of robot that includes four steps: kinematic error modeling, error measurement, kinematic error identification and error compensation [1]. Among these steps, measuring the end-effector pose (i.e., position and orientation) of the robot in the reference coordinate system is a key procedure in robot calibration.

Various measuring devices, such as double ball bar (DBB) [2–4], automatic theodolite [5,6], coordinate measuring machines (CMM) [7–9], FRAO arm [10,11], laser tracker [9,12–14] and customized fixtures [15–17], have been employed for calibration tasks. The DBB is a relative low-cost and off the-shelf device with sub-micro accuracy, thus many researchers have proposed different calibration methods to reduce the kinematic error of various robots by applying this measuring device. Nubiola et al. [2,3] calibrated the kinematic errors of the robot with 6D measurement system based on DBB. The least squares approximation method, Jacobian iteration method and D-HM model had been applied in calibration process. The mean absolute positioning error was improved from 0.873 mm to 0.479 mm after calibrating. Li et al. [18] presented a calibration method for measuring the overconstrained parallel robot using a DBB and a 3-axes linear stage with micrometers. The structural parameters of the robot were identified by the Newton Raphson iteration and least squares method. Accuracy improvements on the order of 90% were achievable after calibration. Gaudreault et al. [19] presented a novel low-cost, three-dimensional automated measuring device and a robot calibration procedure to calibrate a six-axis serial industrial robot. Lee et al. [20] proposed a method to improve the accuracy of machine tools using just a DBB, which was used to measure the length of the six sides of a virtual regular tetrahedron within the workspace. Although these methods greatly improve the motion accuracy of the robot and machine tool, some measurement methods are still complicated, time consuming and small-scale, which are only suitable for the static measurement of robot motion errors. To the best of our knowledge, there has been no research exploring the robot kinematic calibration considering the XY-dimension, continuous

* Corresponding author.
E-mail address: yangp@xmu.edu.cn (P. Yang).

https://doi.org/10.1016/j.precisioneng.2019.12.010
Received 15 May 2019; Received in revised form 17 November 2019; Accepted 28 November 2019
Available online 23 December 2019

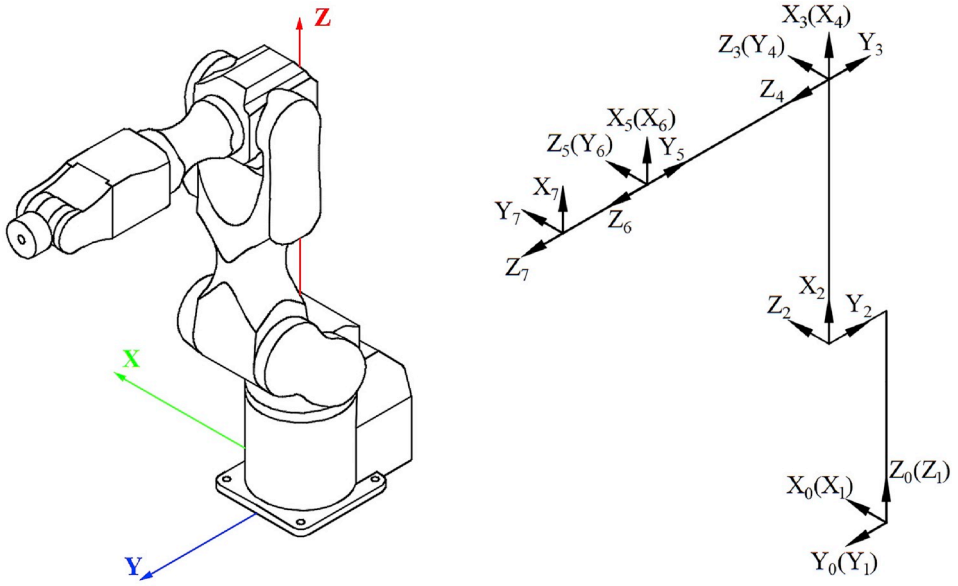

(a) Robot model of EPSON C4-A901 (b) 3D coordinate of each joint of robot

Fig. 1. 3D model of robot and its coordinate system.

Table 1
MDH parameters (unit: angles in rad, lengths in mm,'-' undefined).

i	α_i	a_i	β_i	θ_i	d_i
1	pi/2	100	–	pi/2	320
2	pi	400	0	pi/2	–
3	-pi/2	0	–	0	0
4	pi/2	0	–	0	400
5	-pi/2	0	–	0	0
6	0	0	–	0	150.13

and dynamic measurement. Therefore, a new kinematic calibration method employed DBB as measuring tool is proposed to evaluate the plane motion error of industrial robot, dynamically.

In this paper, the calibration algorithms are combined of MDH method, Jacobian iteration method, the least square method and Newton-Raphson iterative method. Based on the results measured by the DBB, the kinematic error model is established by measuring the roundness error of the circular motion trajectory of the robot. The MDH method is applied to establish the kinematic model of robot. In addition, the Jacobian iteration method is adopted to calculate the error mapping relationship between the motion errors of the end effector and the kinematic parameters errors of each axis. A multi-plane dynamic measurement experiment based on DBB was performed to evaluate the effectiveness of calibration method. To further verify the validity of the calibration method, the laser interferometer was employed to measure the positioning accuracy of end-effector before and after calibration.

2. Robot calibration model based on circular error

2.1. Kinematic model of robot

The EPSON C4-A901 industrial robot shown in Fig. 1a is adopted as a research object. According to Cartesian coordinate, the three-dimensional coordinate of each joint axis is defined as shown in Fig. 1b. Due to the joints 2 and 3 of the robot are linked in parallel, the Modified DH(MDH) model is applied in the study to avoid model singularity [21,22]. 24 kinematic parameters of robot model are described by MDH notion as shown in Table 1. The homogeneous transformation matrix $\boldsymbol{T}$ from the base of the robot to the end-effector of the robot is

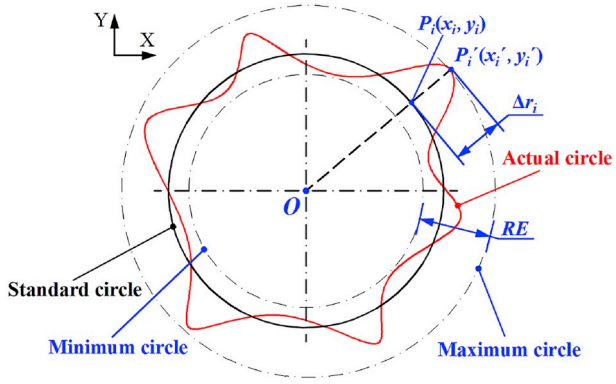

Fig. 2. Measurement error of DBB on the XY plane.

expressed as:

$$\boldsymbol{T} = {}^{0}_{1}\boldsymbol{T}\cdot{}^{1}_{2}\boldsymbol{T}\cdot{}^{2}_{3}\boldsymbol{T}\cdot{}^{3}_{4}\boldsymbol{T}\cdot{}^{4}_{5}\boldsymbol{T}\cdot{}^{5}_{6}\boldsymbol{T}\cdot{}^{6}_{7}\boldsymbol{T} = \prod_{i=1}^{7}{}^{i-1}_{i}\boldsymbol{T} \tag{1}$$

where i-1 $^{i}_{}\boldsymbol{T}$ is the homogeneous transformation matrix from $(i-1)^{\text{th}}$ axis to i^{th} axis.

2.2. Kinematic error model based on circular plane trajectory

The common kinematic mode of the robot in the plane is straight line or curve. In this paper, the circular trajectory is considered as the motion curve to establish the kinematic error model.

The point O (x_0, y_0) of the coordinate system is assumed as the center of the circular trajectory. When the robot moves, the theoretical coordinate of each point is P_i (x_i, y_i). Since the robot has motion error $\boldsymbol{S_i}$, the actual coordinate of the point is $P_i'(x_i', y_i')$ shown in Fig. 2. Then, the kinematic errors of the robot in coordinate system of XOY plane are:

$$\begin{cases} \Delta x_i = x_i^{'} - x_i \\ \Delta y_i = y_i^{'} - y_i \end{cases} \tag{2}$$

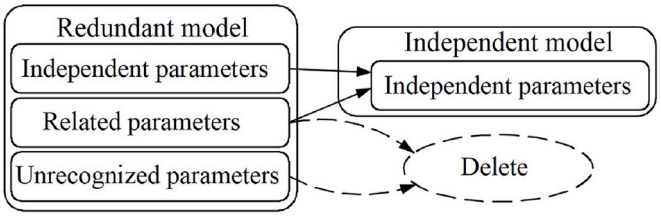

Fig. 3. Schematic diagram for eliminating redundant parameters.

$$\Delta r_i = \sqrt{\Delta x_i^2 - \Delta y_i^2} \tag{3}$$

$\boldsymbol{S_i} = [\boldsymbol{\Delta x_i}\ \boldsymbol{\Delta y_i}]^{\mathrm{T}}$ is the array of motion error that is the difference value between the theoretical position P_i (x_i, y_i) and the actual position $P_i'(x_i', y_i')$.

$$\boldsymbol{S} = \left[\boldsymbol{S}_1\ \boldsymbol{S}_2\ \ldots\ \boldsymbol{S}_{k/2}\right]^T \tag{4}$$

where $\boldsymbol{S}$ is a column vector consisting of $k/2$ motion errors. The evaluation index of the circular plane kinematic accuracy of the robot is roundness error (RE) which is the difference value between the maximum and the minimum values of $\boldsymbol{\Delta r}$ shown as in Fig. 2.

An error mapping relationship between $\boldsymbol{S}$ and the MDH parameter error is established by the Jacobian iterative method. A kinematic model suitable for robot calibration should meet the three principles: Completeness, Continuity and Minimality [23]. Because of the limitation of measurement dimension, the error mapping relationship only indicates the kinematic parameter errors in XY plane. The MDH model is adopted to describe the robot kinematics, while error model based on MDH does not satisfy the minimization criteria. To distinguish MDH parameters, the MDH parameters are classified into three categories:

1) Independent parameters represent that the columns of corresponding Jacobian matrix $\boldsymbol{J}$ are independent of other columns.
2) Related parameters represent that the columns of corresponding Jacobian matrix $\boldsymbol{J}$ are linearly correlated with other columns.
3) Unrecognized parameters represent that the columns of corresponding Jacobian matrix $\boldsymbol{J}$ are all zero.

When the kinematic model is redundant, the identification results of error equation will not converge by applying the least square method. To establish an independent model, the redundant parameters in the redundant model are deleted as shown in Fig. 3. The redundant parameters are including unrecognized parameters and partially related parameters. There are two steps to establish independent model which is only including independent parameters.

Step 1: All zero columns in Jacobian Matrix $\boldsymbol{J}$ are eliminated, that has no effect on the modeling error of the model.
Step 2: The redundant linear correlation columns in Jacobian Matrix $\boldsymbol{J}$ are eliminated.

The robot is described by 24 kinematic parameters which are listed on Table 1. By deleting redundant parameters α_1, α_3, α_4, α_5, d_3, d_4 and d_5, an independent model including 17 independent parameters is obtained to describe the actual planar kinematics of the robot.

2.3. Method of robot calibration

An appropriate kinematic error model is established by selecting the MDH parameters to represent the plane kinematic error of the robot. According to the result from $\boldsymbol{S}$, the observation equation is obtained:

$$\boldsymbol{J\eta} = \boldsymbol{S} \tag{5}$$

$\boldsymbol{J}$ is the Jacobian matrix. Because this study only considered the Cartesian coordinate system in the XOY plane, the equation number of Eq. (5) is $k/2$. k is the element number of $\boldsymbol{S}$ vector. k should be larger than the number of the parameters of independent model.

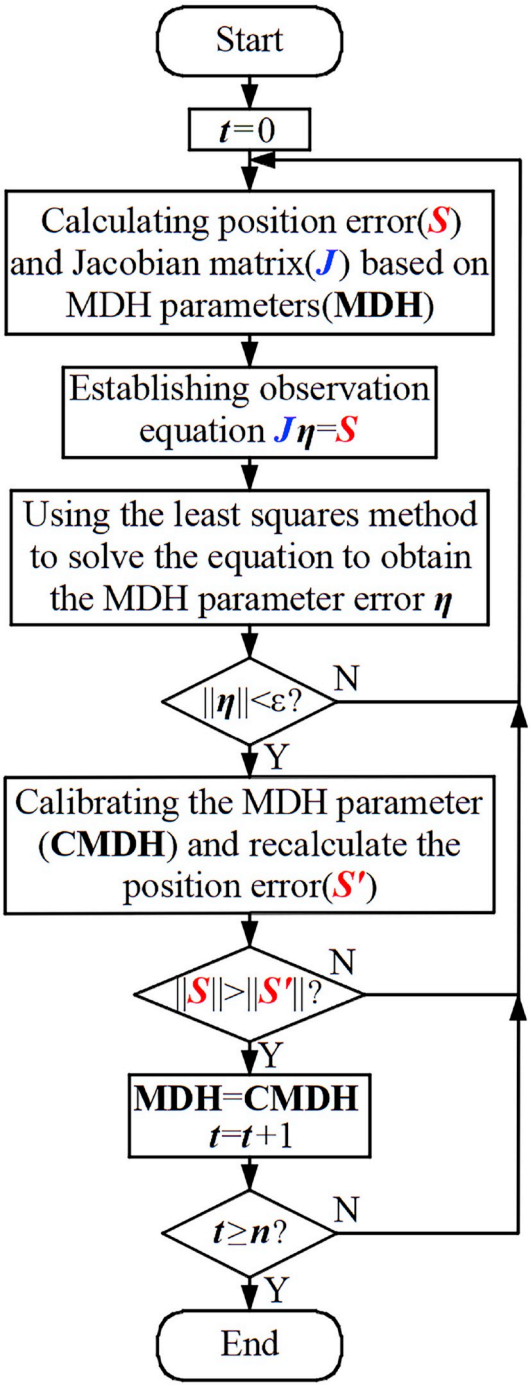

Fig. 4. Flow chart of motion error calibration.

The MDH parameters error are calculated by the least square method [24–26]. The calculation equation of $\boldsymbol{\eta}$ is:

$$\boldsymbol{\eta} = \left(\boldsymbol{J}^T\boldsymbol{J}\right)^{-1}\boldsymbol{J}^T\boldsymbol{S} \tag{6}$$

where $\boldsymbol{\eta}$ is the approximate solution of the MDH parameters error. The validity of the least square solution $\boldsymbol{\eta}$ is determined in two steps:

Table 2
Simulation A1-Given MDH parameters error (unit: lengths in mm, angles in deg).

Category	Distance errors		Angle errors		
	Δa	Δd	$\Delta\alpha$	$\Delta\beta$	$\Delta\theta$
A1-1	0.001		0.001		
A1-2	0.01		0.001		
A1-3	0.1		0.001		

Table 3
Simulation A2-Given MDH parameters error (unit: lengths in mm, angles in deg).

Category	Distance errors		Angle errors		
	Δa	Δd	$\Delta\alpha$	$\Delta\beta$	$\Delta\theta$
A2-1	0.01		0.0001		
A2-2	0.01		0.001		
A2-3	0.01		0.01		

Step 1: If the absolute value of $\boldsymbol{\eta}$ is less than a constraint value ε, move to the next step. Otherwise, $\boldsymbol{\eta}$ need to be recalculated. In this study, the value of ε is setting as 0.01.
Step 2: The position error $\boldsymbol{S}$ and $\boldsymbol{S}'$ are calculated by the MDH model and the calibrated MDH(CMDH) model, respectively. $\boldsymbol{S}'$ is a column vector consisting of motion errors of the end-effector which is calculated by CMDH model. The parameters of CMDH model are calculated by adding $\boldsymbol{\eta}$ to the parameters of the MDH model. If $||\boldsymbol{S}||>||\boldsymbol{S'}||$, the calibration of motion error of robot is acceptable. Otherwise, the calibration is invalid.

The calculation flow chart of motion error calibration is shown in Fig. 4. When $\boldsymbol{\eta}$ is verified, the value of CMDH is assigned to MDH. The algorithm continues to the next cycle until the number of iterations $\boldsymbol{t}$ is larger than or equal to the setting number of iterations $\boldsymbol{n}$. After $\boldsymbol{n}$ times of effective loop iterations, the optimal calibration result is obtained.

Owing to the mechanical design of robot, parts of MDH parameters, such as α, β, a, d, are unable to be modified. Numerous researchers have adopted other methods to compensate the MDH parameter errors by only modifying the joint angle of each axis. Thus, Newton-Raphson iterative method is applied to compensate the angle error in MDH parameter errors [5].

3. Simulation

Because the kinematic error was mainly influenced by the variation of angle error and distance error of each joint, the simulation was divided into two groups to analyze the convergence of the proposed algorithm by setting the parameter errors of different order of magnitude. In the simulation, the three values of angle errors were set as 0.0001°,0.001° and 0.01°, respectively, while the three values of distance errors were set as 1 μm,10 μm and 100 μm, respectively. In the first group of simulation, the value of each angle error was set to a constant under setting the values of the distance errors at different levels (shown in Table 2). In the second group of simulation, the values of distance

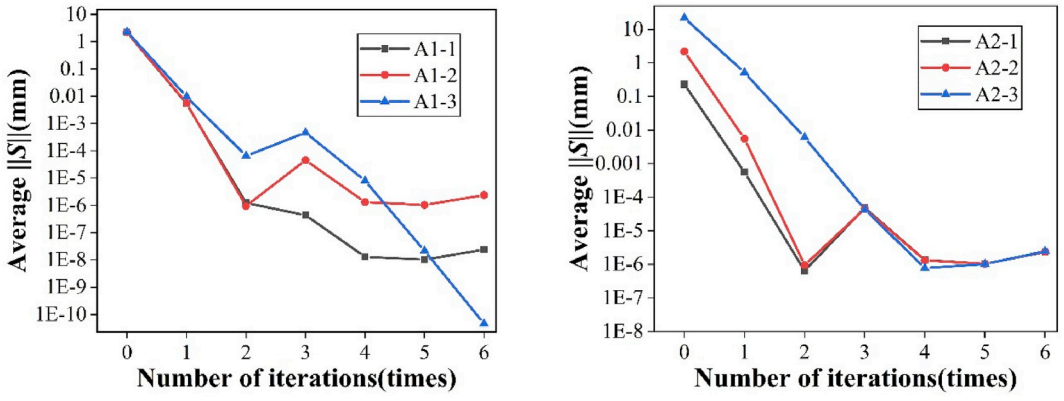

Fig. 5. Simulation results of iterative process.

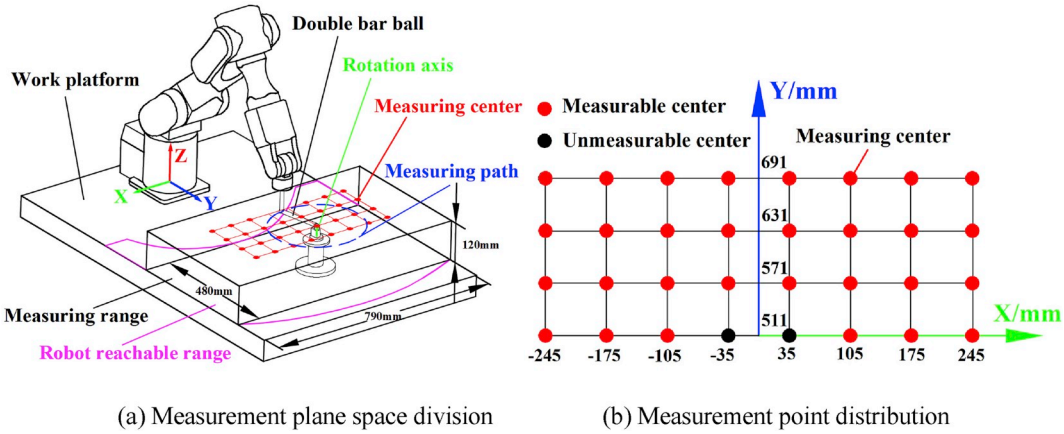

Fig. 6. Measurement plane space division and its distribution.

Table 4
Coordinate distribution of the measuring centers (unit: mm).

Center	1	2	3	4	5	6	7	8	9	10
X	35	35	35	−35	−35	−35	105	105	105	105
Y	571	631	691	571	631	691	511	571	631	691
Z	120	120	120	120	120	120	120	120	120	120
Center	11	12	13	14	15	16	17	18	19	20
X	−105	−105	−105	−105	175	175	175	175	−175	−175
Y	511	571	631	691	511	571	631	691	511	571
Z	120	120	120	120	120	120	120	120	120	120
Center	21	22	23	24	25	26	27	28	29	30
X	−175	−175	245	245	245	245	−245	−245	−245	−245
Y	631	691	511	571	631	691	511	571	631	691
Z	120	120	120	120	120	120	120	120	120	120

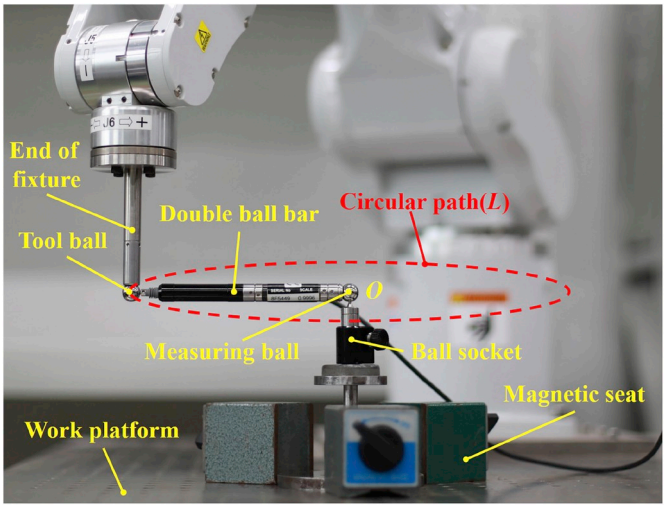

Fig. 7. The installation of the experimental equipment.

errors were set to a constant under setting the value of angle errors at different levels (shown in Table 3).

To observe the iteration effect of the algorithm, the average value of kinematic error modulus of end-effector was adopted to evaluate the iteration effect as shown in Fig. 5. The simulation results in Fig. 5a shows that the average value of kinematic error modulus of end-effector without calibration were 2.1814 mm, 2.1865 mm and 2.2995 mm, respectively. When the number of iterations increased to four times, the average value of modulus decreased to the nanometer level. The simulation results in Fig. 5b shows that the average values of modulus without calibration were 0.2293 mm, 2.1865 mm, and 21.8701 mm, respectively. When the number of iterations increased to three times, the average value of modulus was in the range of nanometer level. The simulation results showed that the method mentioned above had a strong identification effect for the distance and angle parameter errors in different magnitudes.

4. Experiments

4.1. Roundness error evaluation based on multi-plane

Because the robot has larger workspace and greater freedom than the traditional CNC machine, the error characteristics of robots in working area are more complicated. A multi-plane dynamic measurement method based on DBB was proposed to evaluate the distribution characteristics of the kinematic error of the robot in the working plane. The origin of measurement coordinate system coincides with the base coordinate system of robot. The reachable range of the robot is the arc area between the maximum and minimum range of the robot's motion. To ensure that the experiment is carried out in the reachable range of the robot, the measuring region with a size of 480 mm × 790 mm was selected to evaluate the planar motion performance of the robot. The end-effector of the robot can only motion within the reachable range of the robot, as shown in Fig. 6a. The selected plane of the robot was divided into 30 sub-planes, equally. The measuring centers were set at the center of each sub-plane as shown in Fig. 6b. The coordinate distribution of the measuring centers is shown in Table 4. Each measurable center was measured by the DBB with a radius of 150 mm. Roundness error was regarded as an index to evaluate the planar motion accuracy of end-effector of robots.

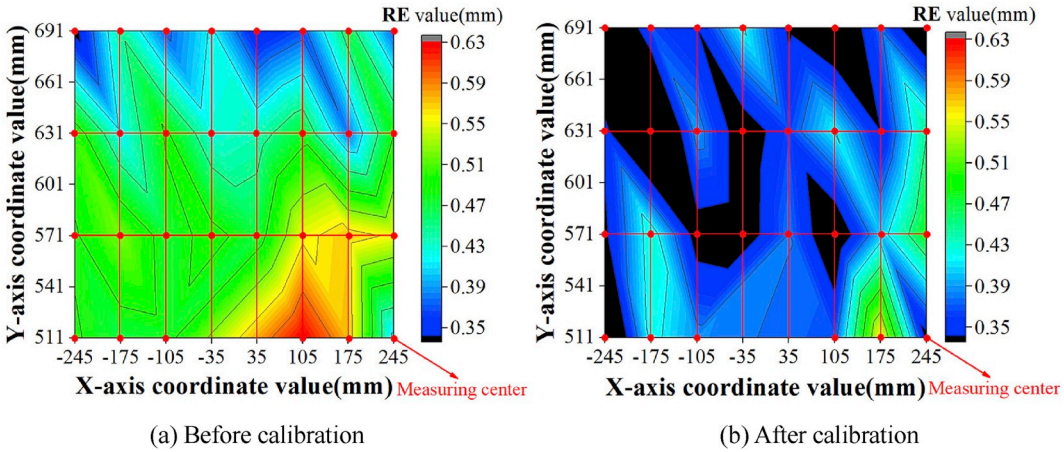

Fig. 8. Distribution of roundness error before and after calibration.

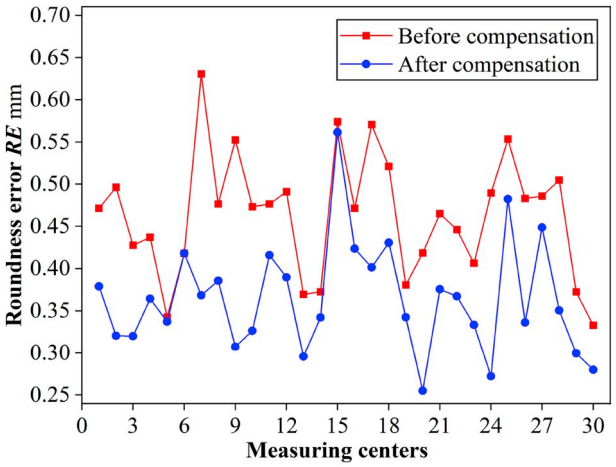

Fig. 9. Comparison of roundness error before and after compensation at multicenter.

The installation of the experimental equipment is shown as in Fig. 7. The measuring ball at the ball socket was fixed at one of the measuring centers in the working area. One end of the DBB was magnetically attracted to the measuring ball. The other end of the DBB was pulled by the end of fixture to rotate around the measuring ball. The radius of rotation was the length of the DBB. The DBB is rotated in the XY plane, thus the coordinate system of the plane was defined as XOY. The initial position of the DBB was in the negative direction of the Y-axis. The DBB obtained the deviation value of rod length measured by the displacement sensor embedded in the rod. The experimental steps were performed as followings:

Step 1: The circular trajectory was defined as *L*. The center of the circle was defined as *O*, while the length of the rod was defined as *r*.
Step 2: The end-effector of the robot was controlled to rotate one turn along the trajectory *L*. The data points measured by the DBB were recorded.

4.2. Experiment results based on DBB

The data of positon error was obtained directly by DBB experiment. The joint angle θ was acquired from the operation software of robot. The CMDH model was established by using the Jacobian iterative algorithm. Then, the Newton-Raphson iterative method was adopted to calculate joint angle errors. Finally, the position information including joint angle errors was fed back to the robot control software. The experiment was re-examined to verify the calibration effect of the method mentioned above.

Considering the measuring radius of the DBB, the measuring region with a size of 180 mm × 490 mm was selected to evaluate the planar motion performance of the robot. Therefore, the variation range of measuring center of DBB is from −245mm to 245 mm in the direction of X axis, while the variation range of measuring center of DBB is from 511 mm to 691 mm in the direction of Y axis. The experiment was performed in 30 sub-planes to evaluate the effectiveness of calibration method. The comparative results before and after compensation are shown in Figs. 8 and 9.

Fig. 8a is mainly in green, which indicates that the results of the roundness error measuring in the workspace were mostly greater than 0.4 mm. Fig. 8b is mostly in blue and black, which shows that the roundness errors were overall less than 0.4 mm after calibration. Comparison of Fig. 8a and b, the roundness error after compensation were significantly lower than that before compensation. 30 groups of comparative experiments were conducted in different locations, which are listed in Table 4. Fig. 9 shows that the roundness error of each sub-planes was improve in different degrees after calibration experiment. Table 5 shows that the average roundness error at 30 sub-planes had dropped about 21.4%, from 0.4637 mm to 0.3644 mm, after calibration. The standard deviation of roundness error was reduced from 0.0720 mm to 0.0656 mm. Thus, it is concluded that the motion accuracy of robot was improved by the proposed calibration method at different central point in plane space.

Table 5
Comparison of roundness error between before and after compensation of multicenter (unit: mm).

Category	Average roundness error	Standard deviation
Before compensation	0.4637	0.0720
After compensation	0.3644	0.0656

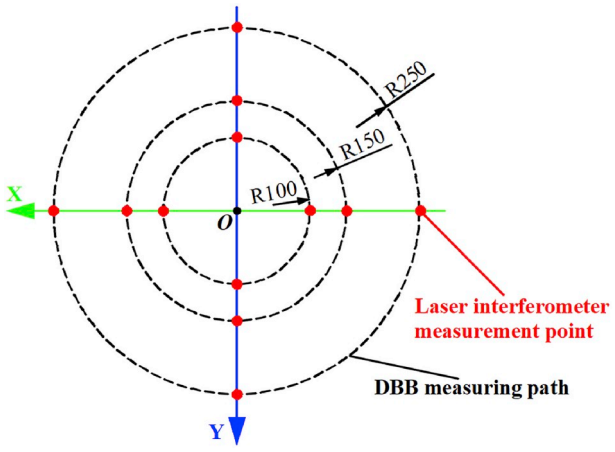

Fig. 10. Measurement positions of Laser interferometer on X and Y axes.

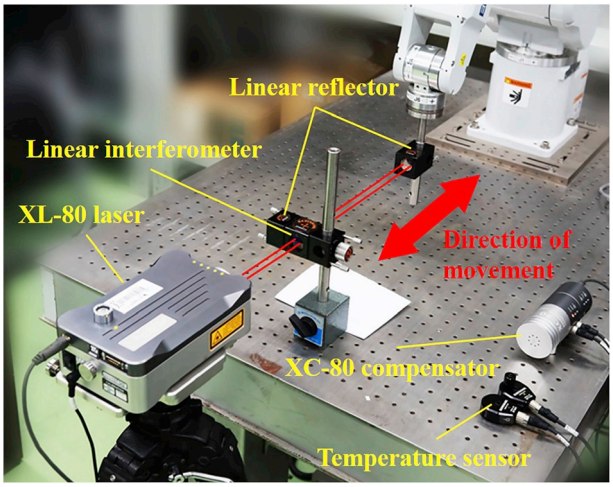

Fig. 11. The installation of the laser interferometer.

4.3. Experimental verification based on laser interferometer

To verify the validity of the calibration method, the laser interferometer was employed to measure the positioning accuracy of end-effector before and after calibration.

In the experiment, the DBB with measuring radius of 100 mm, 150 mm and 250 mm was adopted to calibrate the different size of plane at the same central position, respectively. On the measuring path of the DBB, twelve measuring points were chosen along the X-axis and Y-axis

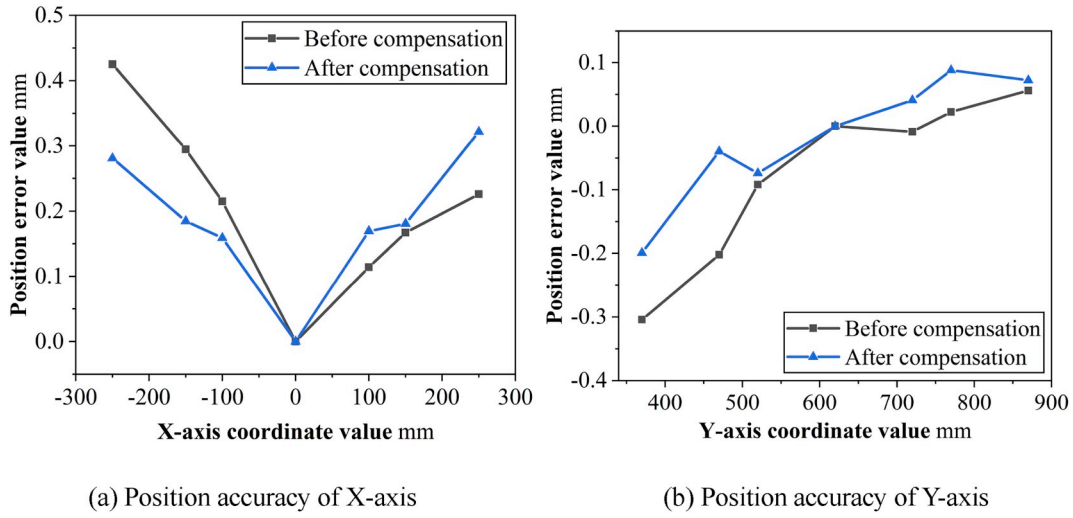

(a) Position accuracy of X-axis (b) Position accuracy of Y-axis

Fig. 12. Comparison of positioning error of end-effector between before and after compensation.

Table 6
Comparison of positioning error between before and after compensation (unit: mm).

Axis	Category	Range	Standard deviation
X	Before-compensation	0.4251	0.1346
	After-compensation	0.3218	0.1025
Y	Before-compensation	0.3603	0.1327
	After-compensation	0.2873	0.0996

directions of the coordinate system, as shown in Fig. 10.

The experimental setup of the laser interferometer in Y direction is shown in Fig. 11 for measuring the same positioning error of the end-effector mentioned above.

To unify the measuring coordinate of the DBB, the measuring origin of the laser interferometer was set as the same center of the DBB. The measurement results of the before and after calibration of each point are shown as in Fig. 12.

The results from Fig. 12 and Table 6 show that the range value of positioning error at X-axis had reduced from 0.4251 mm to 0.3218 mm. The range value of positioning error at Y-axis had reduced from 0.3603 mm to 0.2873 mm. The standard deviation of positioning error at X-axis had dropped from 0.1346 mm to 0.1025 mm. The standard deviation of positioning error at Y-axis had decreased from 0.1327 mm to 0.0996 mm.

5. Conclusions

A new calibration method based on the dynamic measurement of DBB was proposed for improving the kinematic accuracy of industrial robot in circle plane. From the results of simulation and experiment, the followings details were concluded:

(1) The kinematic error model is established by measuring the roundness error of end-effector of robot based on the DBB. The MDH method is applied to establish the kinematic model of robot. The Jacobian iterative method is adopted to create error mapping relationship between the motion error of end-effector and MDH parameters error.
(2) The distance errors and angle errors of each joint axis of robot were simulated by three orders of magnitude respectively, which verifies the identification effect of the proposed algorithm on MDH parameter error. During multiple iterations, the average value of kinematic error modulus of end-effector was reduced to nanometer range.
(3) The average roundness errors of 30 sub-planes in the robot kinematic space calibrated by the proposed method was reduced about 21.4%. Furthermore, the range value of the positioning error acquired from the laser interferometer decreased by 0.1033 mm and 0.0730 mm on the X and Y axis, respectively.

Declaration of competing interest

The authors declare that they have no known competing financial interests or personal relationships that could have appeared to influence the work reported in this paper.

Acknowledgements

This study was supported by the National Natural Science Foundation of China (No. 51975497) and the Natural Science Foundation of Fujian Province, China (Grant No. 2016J01258).

References

[1] Bai Y, Zhuang HQ, Roth ZS. Experiment study of PUMA robot calibration using a laser tracking system. In: Proceedings of the 2003 IEEE international workshop on soft computing in industrial applications; 2003. p. 139–44.
[2] Nubiola A, Bonev IA. Absolute robot calibration with a single telescoping ballbar. Precis Eng 2014;38:472–80.
[3] Nubiola A, Slamani M, Bonev IA. A new method for measuring a large set of poses with a single telescoping ballbar. Precis Eng 2013;37(2):451–60.
[4] Li F, Zeng Q, Ehmann KF, Cao J, Li T. A calibration method for overconstrained spatial translational parallel manipulators. Robot Comput Integr Manuf 2019;57:241–54.
[5] Driels MR, Pathre US. Robot calibration using an automatic theodolite. Int J Adv Manuf Technol 1994;9:114–25.
[6] Sultan IA, Wager JG. Simplified theodolite calibration for robot metrology. Adv Robot 2002;16:653–71.
[7] Driels MR, Swayze W, Potter S. Full-pose calibration of a robot manipulator using a coordinate-measuring machine. Int J Adv Manuf Technol 1993;8:34–41.
[8] Joubair A, Slamani M, Bonev IA. Kinematic calibration of a five-bar planar parallel robot using all working modes. Robot Comput Integr Manuf 2013;29:15–25.
[9] Nubiola A, Slamani M, Joubair A, Bonev IA. Comparison of two calibration methods for a small industrial robot based on an optical CMM and a laser tracker. Robotica 2014;32:447–66.
[10] Wang W, Liu F, Yun C. Calibration method of robot base frame using unit quaternion form. Precis Eng 2015;41:47–54.
[11] Wang W, Wang G, Yun C. A calibration method of kinematic parameters for serial industrial robots. Ind Robot: Int J 2014;41:157–65.
[12] Nubiola A, Bonev IA. Absolute calibration of an ABB IRB 1600 robot using a laser tracker. Robot Comput Integr Manuf 2013;29:236–45.
[13] Yin J, Gao Y. Pose accuracy calibration of a serial five DOF robot. Energy Procedia 2012;14:977–82.

[14] Zhang JB, Wang XB, Wen K, Zhou YH, Yue Y, Yang JZ. A simple and rapid calibration methodology for industrial robot based on geometric constraint and two-step error. Ind Robot 2018;45:715–21.
[15] Joubair A, Bonev IA. Non-kinematic calibration of a six-axis serial robot using planar constraints. Precis Eng 2015;40:325–33.
[16] Zhong XL, Lewis JM, Nagy FLN. Autonomous robot calibration using a trigger probe. Robot Auton Syst 1996;18:395–410.
[17] Joubair A, Bonev IA. Kinematic calibration of a six-axis serial robot using distance and sphere constraints. Int J Adv Manuf Technol 2015;77:515–23.
[18] Li F, Zeng Q, et al. A calibration method for overconstrained spatial translational parallel manipulators. Robot Comput Integr Manuf 2019;57:241–54.
[19] Gaudreault M, Joubair A, Bonev I. Self-calibration of an industrial robot using a novel affordable 3D measuring device. Sensors 2018;18(10):3380.
[20] Lee KI, Lee HH, Yang SH. Interim check and practical accuracy improvement for machine tools with sequential measurements using a double ball-bar on a virtual regular tetrahedron. Int J Adv Manuf Technol 2017;93(5–8):1527–36.
[21] Denavit J, Hartenberg RS. A kinematic notation for lower-pair mechanisms based on matrices. Trans ASME J Appl Mech 1955;22:215–21.
[22] Veitschegger WK, Wu CH. Robot accuracy analysis based on kinematics. IEEE Trans Robot Autom 1986;2:171–9.
[23] Zhang XC, Song YT, Yang Y, Pan HT. Stereo vision based autonomous robot calibration. Robot Auton Syst 2017;93:43–51.
[24] Levenberg K. A method for the solution of certain non-linear problems in least squares. Q Appl Math 1944;2:164–8.
[25] Antonelli G, Chiaverini S, Fusco G. A calibration method for odometry of mobile robots based on the least-squares technique: theory and experimental validation. IEEE Trans Robot 2005;21:994–1004.
[26] Veitschegger WK, Wu CH. Robot calibration and compensation. IEEE Trans Robot Autom 1988;4:643–56.